Article

Quantitative contributions of TNF receptor superfamily members to CD8^{+} T-cell responses

John Nguyen, Johannes Pettmann, Philipp Kruger & Omer Dushek [iD]

Abstract

T-cell responses to infections and cancers are regulated by co-signalling receptors grouped into the binary categories of co-stimulation or co-inhibition. The co-stimulation TNF receptor superfamily (TNFRSF) members 4-1BB, CD27, GITR and OX40 have similar signalling mechanisms raising the question of whether they have similar impacts on T-cell responses. Here, we screened for the quantitative impact of these TNFRSFs on primary human CD8^{+} T-cell cytokine production. Although both 4-1BB and CD27 increased production, only 4-1BB was able to prolong the duration over which cytokine was produced, and both had only modest effects on antigen sensitivity. An operational model explained these different phenotypes using shared signalling based on the surface expression of 4-1BB being regulated through signalling feedback. The model predicted and experiments confirmed that CD27 co-stimulation increases 4-1BB expression and subsequent 4-1BB co-stimulation. GITR and OX40 displayed only minor effects on their own but, like 4-1BB, CD27 could enhance GITR expression and subsequent GITR co-stimulation. Thus, different co-stimulation receptors can have different quantitative effects allowing for synergy and fine-tuning of T-cell responses.

Introduction

T cells are critical mediators of adaptive immunity against pathogens and tumours. Their activity is primarily controlled by the T-cell receptor (TCR) that recognises peptide antigens bound to major histocompatibility complexes (pMHCs) presented on antigen-presenting-cells (APCs). Binding of pMHC to the TCR can transduce signalling that can activate T cells to initiate, regulate and maintain immune responses (Smith-Garvin *et al*, 2009; van der Merwe & Dushek, 2011). Although TCR signalling is required for this process, a range of other co-signalling receptors are also known significantly

modulate the TCR signal and hence T-cell activity (Chen & Flies, 2013). Depending on their overall positive or negative impact on T-cell activity, these co-signalling receptors have been binarily divided into co-stimulatory (e.g. CD28 and 4-1BB) or co-inhibitory receptors (such as CTLA-4 and PD-1). Many of these receptors fall into the immunoglobulin and tumour necrosis factor receptor superfamilies (IgSF and tumour necrosis factor receptor superfamily [TNFRSF], respectively) which differ in structure and signalling mechanisms. Even within these families, the expression patterns and functional phenotypes of these receptors display large variation. Despite these differences, our classification of these co-signalling receptors has largely been confined to the binary qualitative categories based on whether ligation of a co-signalling receptor increases (co-stimulatory) or decreases (co-inhibitory) T-cell responses.

Critically important quantitative features of a T-cell function such as cytokine production and target killing) include rate (Fig. 1A), sensitivity (Fig. 1B), and duration of the response (Fig. 1C). For example, increases in the rate of cytokine production in response to a certain amount of presented antigen have been demonstrated for the archetypal co-stimulatory receptor CD28 (Langenhorst *et al*, 2018). Enhanced sensitivity, on the other hand, would allow T cells to respond to lower doses of antigen, which is well-established for adhesion receptors (e.g. CD2 and LFA-1) (Koyasu *et al*, 1990; Bachmann *et al*, 1997; Bachmann & Ohashi, 1999), although this also appears to be the case for CD28 to some extent (Viola & Lanzavecchia, 1996; Zhang *et al*, 2002). Finally, it has been shown in multiple *in vitro* and *in vivo* systems that T cells exhibit adaptation so that they produce cytokine for limited duration to a constant dose of antigen (Singh & Schwartz, 2003; Stamou *et al*, 2003; Han *et al*, 2010), and this duration can be controlled by co-signalling receptors (Trendel *et al*, 2021). Existing evidence suggests that co-stimulatory TNFRSF members may increase the rate of the response (Gramaglia *et al*, 1998; Choi *et al*, 2011; Ramakrishna *et al*, 2015), but their impact on sensitivity and duration of the T-cell response is poorly characterised. Quantitative differences in T-cell responses may provide a rationale for why similar surface receptors are expressed on the same T-cell population.

Here, we focus on TNF receptor-associated factor (TRAF)-binding receptors of the TNFRSF, with 4-1BB (CD137), CD27, OX40 (CD134) and GITR (AITR, CD357) as well-established representative co-stimulatory receptors on T cells. Their signalling mechanisms and components of their molecular pathways have been characterised in great detail (Watts, 2005; Zapata *et al*, 2018). At the same
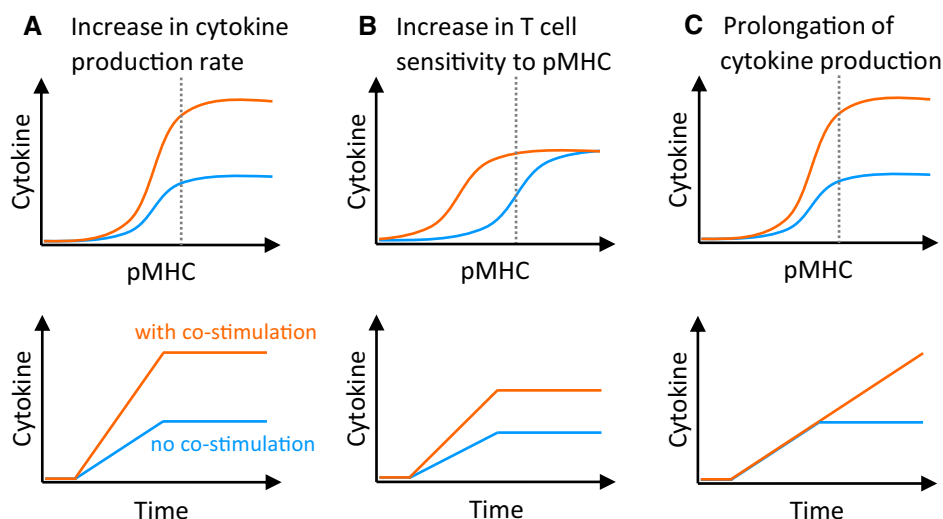
Sir William Dunn School of Pathology, University of Oxford, Oxford, UK
*Corresponding author. Tel: +44 1865 275576; E-mail: omer.dushek@path.ox.ac.uk

Figure 1. Quantitative effects of co-stimulation on the T-cell cytokine response.

A–C Graphical representation of hypothetical co-stimulation affecting the (A) rate, (B) sensitivity and (C) duration of the T-cell cytokine response, shown as pMHC dose response at the endpoint (top row) and time courses at the pMHC dose indicated by the dotted line (bottom row). The *y*-axis represents the cumulative amount of cytokine produced. Blue and orange lines represent the cytokine response in the absence and presence of co-stimulation, respectively.

time, a range of functional data has been collected for these receptors in various *in vitro* and *in vivo* systems and in the clinic (Ward-Kavanagh *et al*, 2016), often focusing on qualitative features of co-stimulation such as enhanced T-cell proliferation, survival, anti-viral or anti-tumour response, differentiation and memory formation. This wealth of information is now being utilised for the development of biotherapeutics targeting TNFRSF members (Schaer *et al*, 2014), as well as adoptive cell therapies for the treatment of cancers using T cells engineered with mechanisms to activate their pathways (Weinkove *et al*, 2019). Despite previous breakthroughs (Locke *et al*, 2019), these promising endeavours are often impeded by modest performance in clinical trials (Tolcher *et al*, 2017; Ansell *et al*, 2020; Wagner *et al*, 2020). Although our molecular understanding of these receptors is mature, our understanding of how these receptors quantitatively shape T-cell functions, including their ability to control the rate and duration of cytokine production, and their impact on antigen sensitivity, is underexplored. This quantitative understanding of how receptors control cellular function has been referred to as an "operational" understanding and can be used to develop operational mathematical models that be constructed to predict how receptor inputs control downstream cellular outputs (Antebi *et al*, 2017). These models can improve our ability to operate T cells for therapies.

Using primary human CD8$^+$ T cells, we systematically explored the impact of TNFRSF co-stimulation on quantitative T-cell responses. We found that 4-1BB and CD27 increased the rate of cytokine production but only 4-1BB could also prolong the duration, and both receptors had only a modest impact on antigen sensitivity. Ligands to GITR and OX40 had only modest effects, possibly due to their relatively low expression on CD8$^+$ T cells. The systematic quantitative data allowed us to construct a mathematical model that reconciled these different phenotypes with their largely shared signalling mechanisms by relying on differences in the regulation of

surface receptor expression. This operational model predicted a synergy between the receptors based on feedback control of surface expression of inducible TNFRSF members, and we confirmed this to be the case by showing that CD27 co-stimulation improved subsequent co-stimulation not only by 4-1BB, but also by GITR. The work highlights how T-cell co-stimulation even by similar surface receptors can exhibit differences in quantitative responses and synergy.

Results

Co-stimulation through TNFRSF members produces quantitatively different phenotypes

To quantitatively study TNFRSF co-stimulation, we first isolated, *in vitro* expanded and transduced primary human CD8$^+$ T cells with the c58c61 TCR (Li *et al*, 2005) using a standard adoptive T-cell therapy protocol (Rapoport *et al*,2015). This protocol produces T-cell blasts, which serve as a model for *in vivo* generated effector T cells, able to kill target cells and rapidly secrete cytokines. The c58c61 affinity-enhanced TCR recognises the cancer-testes antigen NY-ESO-1$_{157-165}$ on HLA-A2, of which we used a variant with physiological affinity (K_D = 1.78 µM (Lever *et al*, 2016), see also Materials and Methods). To precisely control pMHC antigen and TNFRSF ligand dose and duration of stimulation (Iezzi *et al*, 1998), these T cells were presented with recombinant ligands on plates (Aleksic *et al*, 2010; Dushek *et al*, 2011; Lever *et al*, 2016; Abu-Shah *et al*, 2020) (Fig. 2A). We systematically stimulated T cells with 12 doses of pMHC and 3–7 doses of trimeric ligands to four members of the TNFRSF; 4-1BB, CD27, GITR and OX40, to study the impact of TNFRSF co-stimulation on quantitative T-cell responses. By measuring T-cell responses at four different time points, we generated a dataset with 1,056 independent conditions (Fig. 2B). This allowed

us to accurately determine the maximal efficacy of cytokine production (E_{max}, maximal response across different antigen doses) and antigen sensitivity (EC_{50}, antigen dose at which half-maximal response is observed) at different time points.

As we previously found (Trendel *et al*, 2021), presentation of antigen in the absence of co-stimulation induced a burst of cytokine but ultimately led to adaptation, whereby T cells stopped cytokine production so that supernatant levels remained similar after 8 h (Fig. 2B, grey line). This is observed by the constant value of E_{max} (Fig. 2C) or by the rate of change of E_{max} approaching 0 (Fig. 2D) after 8 h without co-stimulation.

Simultaneous engagement of TCR and these co-stimulatory receptors revealed different quantitative phenotypes (Fig. 2B). We found that 4-1BB co-stimulation had the strongest amplification on cytokine production, and this amplification continued to increase over time beyond 8 h with the maximum cytokine production observed at the final time point (Fig. 2C). This was achieved by maintaining a high rate of cytokine production (Fig. 2D). Although CD27 co-stimulation amplified cytokine production, it appeared to be less effective at halting adaptation so that the amplification remained similar after 8 h with the rate of change of cytokine production decreasing after this time (Fig. 2B–D). We observed similar effects on TNF and IL-2 production (Appendix Fig S1), although IL-2 levels decreased over time, which is likely a result of consumption (discussed further below). In comparison, GITR and OX40 had almost no effect on cytokine production (Fig 2B–D). Together, these data suggested that the effect of CD27 co-stimulation is rather front-loaded, i.e. increasing the early response within the first 8 h only, whereas 4-1BB co-stimulation is most effective at later time points when T cells without co-stimulation would already halt their response.

This pattern of cytokine production was consistent with the temporal expression pattern of these receptors (Fig 2E), with CD27 being highly expressed on resting T cells and rapidly downregulated upon engagement with its ligand CD70, while 4-1BB is not present on resting T cells and only upregulated upon TCR-dependent activation. This activation-induced expression of 4-1BB appears to somewhat compensate for the 4-1BBL-induced downregulation of the receptor, allowing it to remain on the cell surface for longer, possibly resulting in the more persistent effect of 4-1BB co-stimulation. GITR and OX40 are similarly activation-induced, however, with much slower kinetics and reaching lower levels compared with 4-1BB on CD8^{+} T-cell blasts (Appendix Fig S2), which could explain their weak effects in our system. These receptors are likely more relevant on other T-cell populations, such as those among CD4^{+} T cells (Serghides *et al*, 2005; Yu *et al*, 2006; Clouthier *et al*, 2015). Therefore, our further analysis mostly focused on CD27 and 4-1BB.

In addition to impacting the rate and duration of cytokine production, TNFRSF co-stimulation also appeared to enhance the T-cell sensitivity to pMHC antigen. We observed that 4-1BBL or CD70 co-stimulation led to a 2- to 10-fold lower EC_{50} (Appendix Fig S3). Once again, the timing of these effects matched the expression pattern of the co-stimulatory receptors: the EC_{50} initially remained unaffected by 4-1BB co-stimulation and gradually decreased over time in comparison with the control without co-stimulation (Appendix Fig S3A and B), while the effect of CD70 was largest at the earlier time points and is appreciably reduced by 24 h (Appendix Fig S3C and D). While the effects of 4-1BB and CD27 on T-cell

sensitivity are statistically significant, they are dwarfed by those of adhesion receptors such as CD2 (Koyasu *et al*, 1990; Bachmann & Ohashi, 1999), for which we observe up to several hundred-fold reduction in EC_{50} in our system (Appendix Fig S3E). Therefore, we focused on understanding their impact on rate and duration of cytokine production.

Cytokine response in adapted T cells can be rescued by co-stimulation through TNFRSF

In the previous experiments, TNFRSF co-stimulation was provided at the outset. This raises the question of whether TNFRSF co-stimulation can revert T-cell adaptation once it has already been established.

While CD27 co-stimulation was not able to prevent adaptation in the time course experiments (Fig 2), under the assumption that this is merely due to rapid downregulation of CD27, preserving CD27 expression on adapted T cells may render them receptive to CD70-induced rescue of cytokine responses. To study this, we pre-stimulated T cells with a dose response of pMHC alone for 16 h to induce unresponsiveness. Transferring these pre-treated cells to the same dose range of pMHC alone for another 8 h resulted in only modest cytokine production, confirming that these T cells had adapted to the antigen dose they experienced in the first stimulation. Engaging CD27 in this second stimulation could indeed rescue the cytokine response confirming that CD27 can rescue adapted T cells (Fig 3A–E). In addition, the presence of CD70 in the first stimulation did not prevent unresponsiveness to pMHC alone in the second stimulation confirming that CD27 cannot override adaptation. Moreover, it rendered CD27 co-stimulation in the second phase less effective, which is expected due to the early downregulation of CD27 by CD70 in the first stimulation. Taken together, ligation of CD27 can revert T-cell adaptation in a pMHC-dependent manner once it is established provided that CD27 has not been downregulated.

Although GITR co-stimulation produced only modest increases in cytokine production in the time course, we found that in this two-phase experiment, it was able to partially revert unresponsiveness in pre-stimulated T cells (Appendix Fig S4). This might have been due to the small effect of GITR being masked by the early co-stimulation-independent burst of cytokine in the time course experiments. We noted that unlike IFN-γ and TNF, GITR co-stimulation could not rescue the IL-2 response in these plate-transfer experiments and this could be explained by the ability of T cells to consume IL-2 (Appendix Fig S4C). T cells indeed upregulated CD25 upon activation in our system (Appendix Fig S6A), which is part of the high-affinity IL-2 receptor (Wang *et al*, 2005; Stauber *et al*, 2006).

We have recently shown that 4-1BB engagement can rescue cytokine responses from adapted T cells (Trendel *et al*, 2021), albeit using different stimulation times. We therefore repeated the experiments using the timings above for CD27 and GITR and confirmed that delaying 4-1BB engagement can rescue cytokine responses (Appendix Fig S5A–C). Given that 4-1BB expression is induced by pMHC-dependent TCR signalling, we could not rule out that 4-1BB expression alone was sufficient to induce cytokine production (i.e. that T cells were now licenced to secrete cytokine independent of pMHC) because in conditions without pMHC or with low doses of pMHC in the second stimulation phase, 4-1BB was not expressed. Therefore, in a second set of experiments, the T cells were all pre-
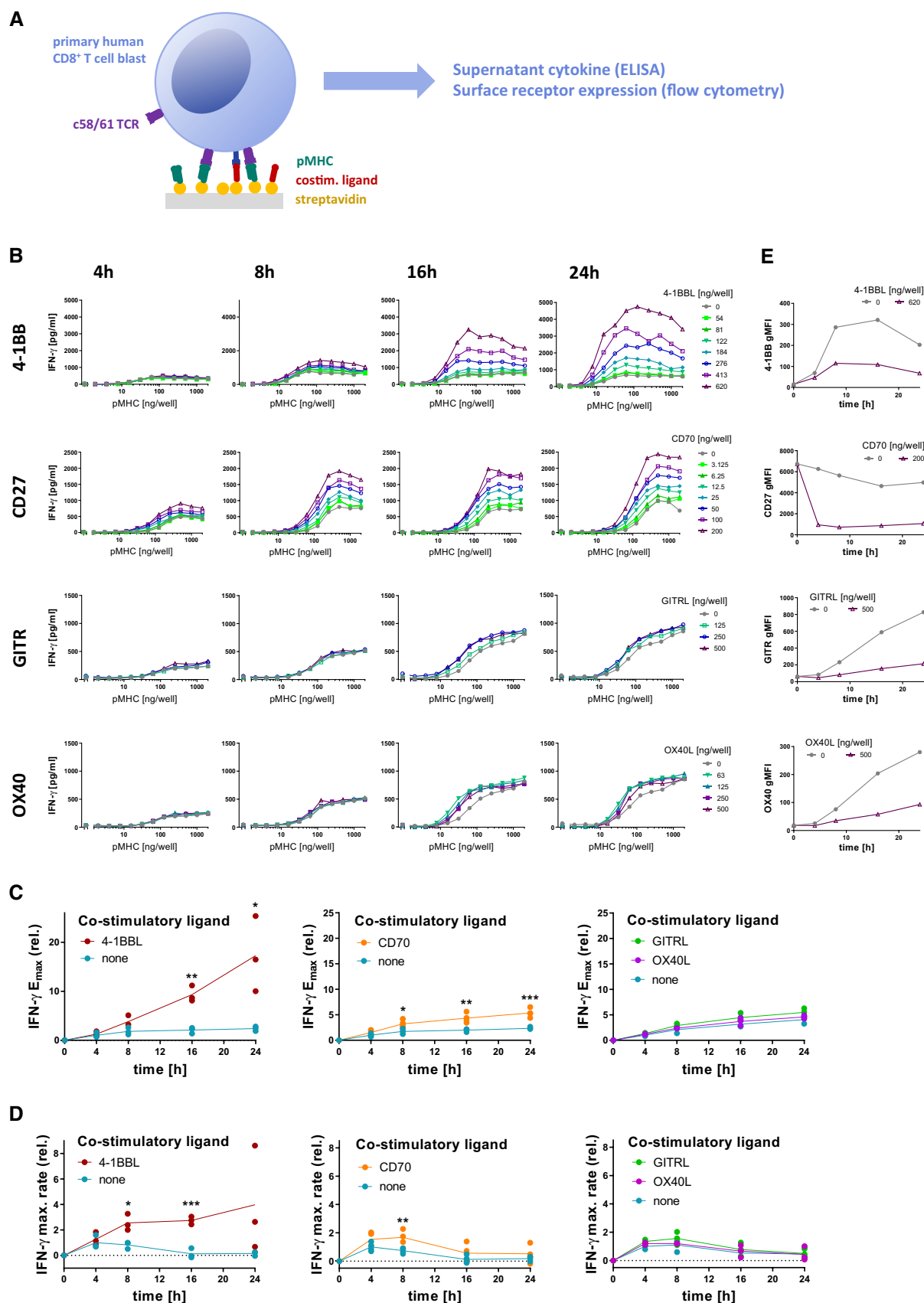
Figure 2.

◀

Figure 2.   CD8$^+$ T-cell co-stimulation through different TNFRSF members produces quantitatively different IFN-γ cytokine phenotypes.

A   Primary human CD8$^+$ T cells transduced with the c58/c61 TCR were stimulated for 4, 8, 16 and 24 h with plate-immobilised pMHC and ligands to TNFRSF members at the indicated doses. The production of cytokines into the culture medium supernatant was quantified by ELISA. Surface receptors were labelled with fluorescent antibodies and quantified by flow cytometry.
B   Representative IFN-γ dose responses for the four measured time points, with different colours representing the indicated doses of TNFSF ligands.
C   Cytokine E_{max} values normalised to E_{max} without co-stimulation at 4 h (three independent experiments).
D   Rate of change of E_{max} from (C) normalised to the rate without co-stimulation at 4 h. The rate is taken to be 0 at 0 h.
E   Representative surface expression time courses of TNFRSF members on cells stimulated with 2,000 ng/well pMHC, with or without the respective ligands.

Data information: E$_{max}$ values and rates of cytokine production with and without co-stimulation were compared using multiple two-tailed t-tests. *P-value < 0.05; **P-value < 0.01; ***P-value < 0.001.

stimulated with a fixed dose of pMHC and CD70 for 16 h to uniformly induce high 4-1BB expression with minimal TCR downregulation before transferring them to a dose range of pMHC, with or without 4-1BBL, for another 8 h (Appendix Fig S5D–F). The pMHC dose dependency of the cytokine response in the second phase indicated that cytokine production was still strictly dependent on TCR stimulus, since at low pMHC doses (or at no pMHC), no response was observed despite high 4-1BB expression and 4-1BBL availability (red and orange lines), confirming 4-1BB as a bona-fide co-stimulatory receptor incapable of inducing a T-cell response on its own.

The validity of conclusion drawn from these plate-transfer experiments hinges on a high standard of reproducibility of plate coatings and the maintenance of a constant pMHC stimulus. To demonstrate this, we quantified the coated amount of pMHC on the plates using an immunofluorescence assay, both before addition of cells (with or without the cognate TCR) and after a 16-h stimulation phase and harvest of the cells for the transfer. No changes in coating were detected between the different conditions, indicating that the pMHC is not decaying or consumed at any rate relevant to the time scale of our experiments (Appendix Fig S6B). Moreover, viability staining of the cells after the entire process of the experiment shown in Appendix Fig S5D–F shows that the unresponsiveness of adapted T cells was not due to cell death (Appendix Fig S6C), in addition to the fact that their response could be rescued with 4-1BB co-stimulation.

Taken together, co-stimulation by 4-1BB, CD27 and GITR can rescue cytokine production in a pMHC-dependent manner by unresponsive T cells. This is consistent with their shared signalling pathways (Watts, 2005) and supports the hypothesis that differences in their quantitative phenotypes are a result of surface receptor expression and regulation.

A mechanistic model reproduces the different TNFRSF co-stimulation phenotypes based on shared signalling but different feedback controls of receptor expression

We have previously published a simple mechanistic mathematical model which could explain T-cell adaptation as a consequence of TCR downregulation (Trendel *et al*, 2021). This ordinary differential equation (ODE) model included pMHC binding to the TCR that induced both TCR downregulation and TCR signalling (effectively an incoherent feedforward loop) that could turn on a digital switch that activated downstream signalling leading to cytokine production (Fig 4A).

We next systematically explored where in this pathway can 4-1BB and CD27 integrate their signals to reproduce the cytokine data we had collected (Appendix Figs S7 and S8). For example, we found that if CD27 and 4-1BB modulated the pMHC-TCR interaction, they

would only shift the dose–response EC_{50} in our model and leave the large changes in cytokine production rate and duration unexplained (Appendix Fig S7A). We could reproduce the changes in cytokine production by allowing them to modulate TCR expression and downregulation but this required that CD27 and 4-1BB co-stimulation increase surface TCR levels. However, measurements of TCR surface expression show rather the opposite, i.e. a 4-1BBL and CD70 dose-dependent enhancement of TCR downregulation (Appendix Fig S7B), possibly as a result of their modest abilities to increase adhesion to the stimulation surface. Using data from Fig 3B and C, we were also able to exclude five alternative models with downstream integration points which were inconsistent with our observations (Appendix Fig S8).

This process of elimination led us to a single model that can explain the cytokine data based on 4-1BB and CD27 signalling modulating the molecular switches that convert the analogue antigen signal into the reported digital cytokine response on single cell level (Bucy *et al*, 1994; Huang *et al*, 2013) (see Fig 4A). Simulation of a time course using this model, with the co-stimulatory receptor being present from the start and rapidly downregulated upon engagement, was able to reproduce the CD27 co-stimulation phenotype with an increased rate of initial cytokine production but eventual arrest of the response within the same time scale of T-cell adaptation in the absence of co-stimulation (Fig 4B–D). In the case of 4-1BB, with the co-stimulatory receptor being absent on resting cells and induced upon activation, the model was also able to replicate the longer duration and hence higher rate of cytokine production at time points after 8 h.

In summary, our mechanistic model confirmed that the difference in receptor expression is sufficient to explain the divergent phenotypes of CD27 and 4-1BB co-stimulation (Fig 4D) when they share the same signalling mechanism. In contrast to CD27 which is short-lived due to ligand-induced downregulation, 4-1BB co-stimulation is sustained through a feedback loop which replenishes surface 4-1BB expression by activation-induced synthesis of 4-1BB.

Sequential engagement of CD27 and 4-1BB produces synergistic effects

The operational model that we inferred from our data predicted synergy between CD27 and 4-1BB. This prediction is based on the inference that CD27 integrates its signal within the positive feedback that drives 4-1BB surface expression (Fig 4A). Thus, the model suggests that CD27 would not only increase cytokine production directly but also increase 4-1BB expression and therefore, improve the subsequent co-stimulation effects induced by 4-1BB
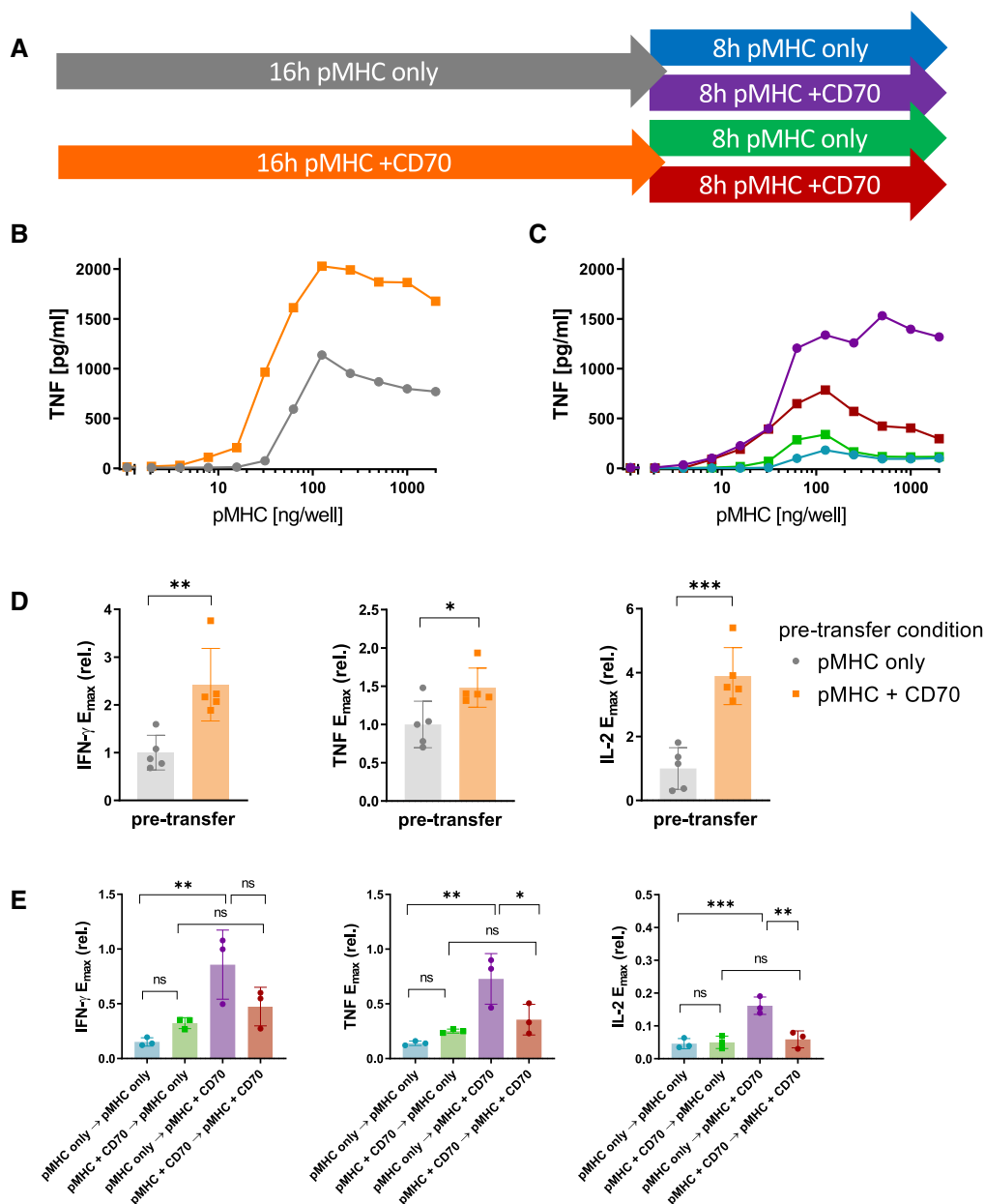
Figure 3. CD27 co-stimulation is capable of rescuing the cytokine response in already adapted T cells if not engaged during the first stimulation.

A   Primary human CD8^{+} T cells transduced with the c58/c61 TCR were stimulated for 16 h with pMHC doses varying from 0 to 2,000 ng/well in the presence or absence of 200 ng/well CD70. Cells were harvested, washed and stimulated for further 8 h with identical pMHC doses which they were adapted to, with or without addition of 200 ng/well CD70. The production of the cytokines IFN-γ, IL-2 and TNF into the culture medium supernatant was quantified by ELISA.

B   T-cell response during the first 16-h stimulation from one representative experiment.

C   T-cell response during the secondary 8-h stimulation from the same experiment.

D, E E_{max} values from three independent experiments were extracted from dose–response curve fits and normalised to the cytokine response during the 16 h pre-stimulation without co-stimulation (mean ± SD). Pre-transfer conditions (pMHC with or without CD70) in (D) were compared with a two-tailed t-test. Conditions in (E) were compared using one-way ANOVA with Šídák's correction for multiple comparisons. ns = P-value > 0.05; *P-value < 0.05; **P-value < 0.01; ***P-value < 0.001.

engagement. We illustrated this by simulating the two-phase stimulation assay, whereby T cells were stimulated with a dose range of pMHC with or without addition of CD70 for 16 h, followed by a transfer to the same pMHC doses in the absence or presence of 4-1BBL (Fig 5A). Not only does CD27 co-stimulation increase cytokine production in the first phase as shown previously (Figs 2 and 3B); the model additionally predicted that 4-1BB surface expression would be elevated, and the amount of cytokine produced during the second stimulation would also be increased in the presence of 4-1BBL (Fig 5B). These predictions were confirmed experimentally
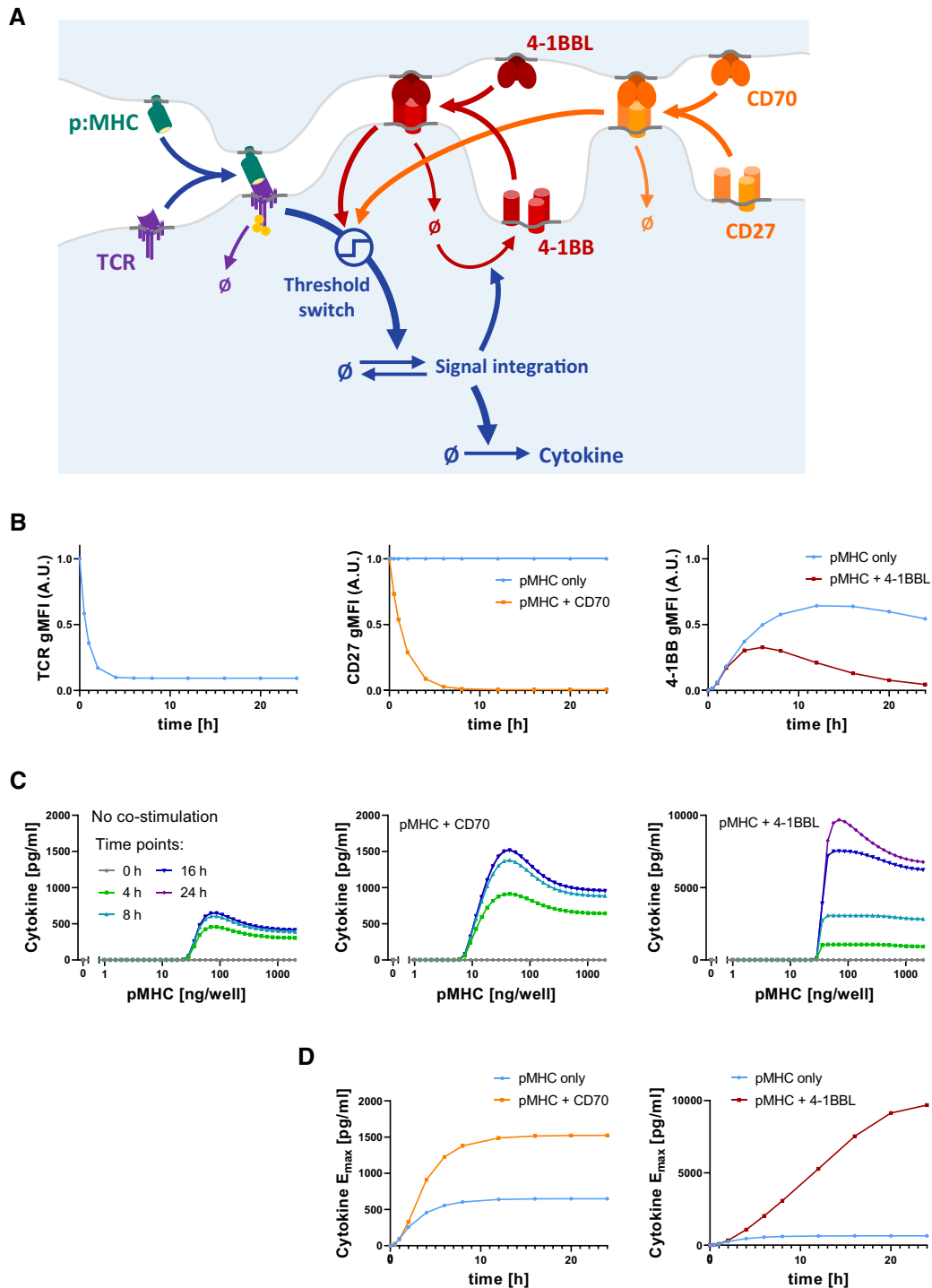
Figure 4. An operational mathematical model explains the divergent phenotypes of 4-1BB and CD27 based on a shared signalling mechanism but different surface receptor regulation.

A Model schematic: T-cell receptor (TCR) and peptide-major histocompatibility complex (pMHC) form a receptor–ligand complex that induces the cytokine response, gated by a threshold switch. At the same time, ligand binding causes downregulation of the TCR. Similarly, the co-stimulatory TNFRSF/TNFSF receptor–ligand pair forms a complex which causes modulation of the T-cell activation threshold, as well as downregulation of the TNFRSF. In the case of CD27, the receptor is present from the start, whereas 4-1BB expression is induced by TCR signalling.

B Simulated time courses of TCR (left), CD27 (middle) and 4-1BB (right) surface expression using the model in (A) for pMHC in the absence or presence of the respective TNFRSF ligands.

C Simulated cytokine dose responses for the indicated time points in the absence (left) or presence of CD70 (middle) or 4-1BBL (right).

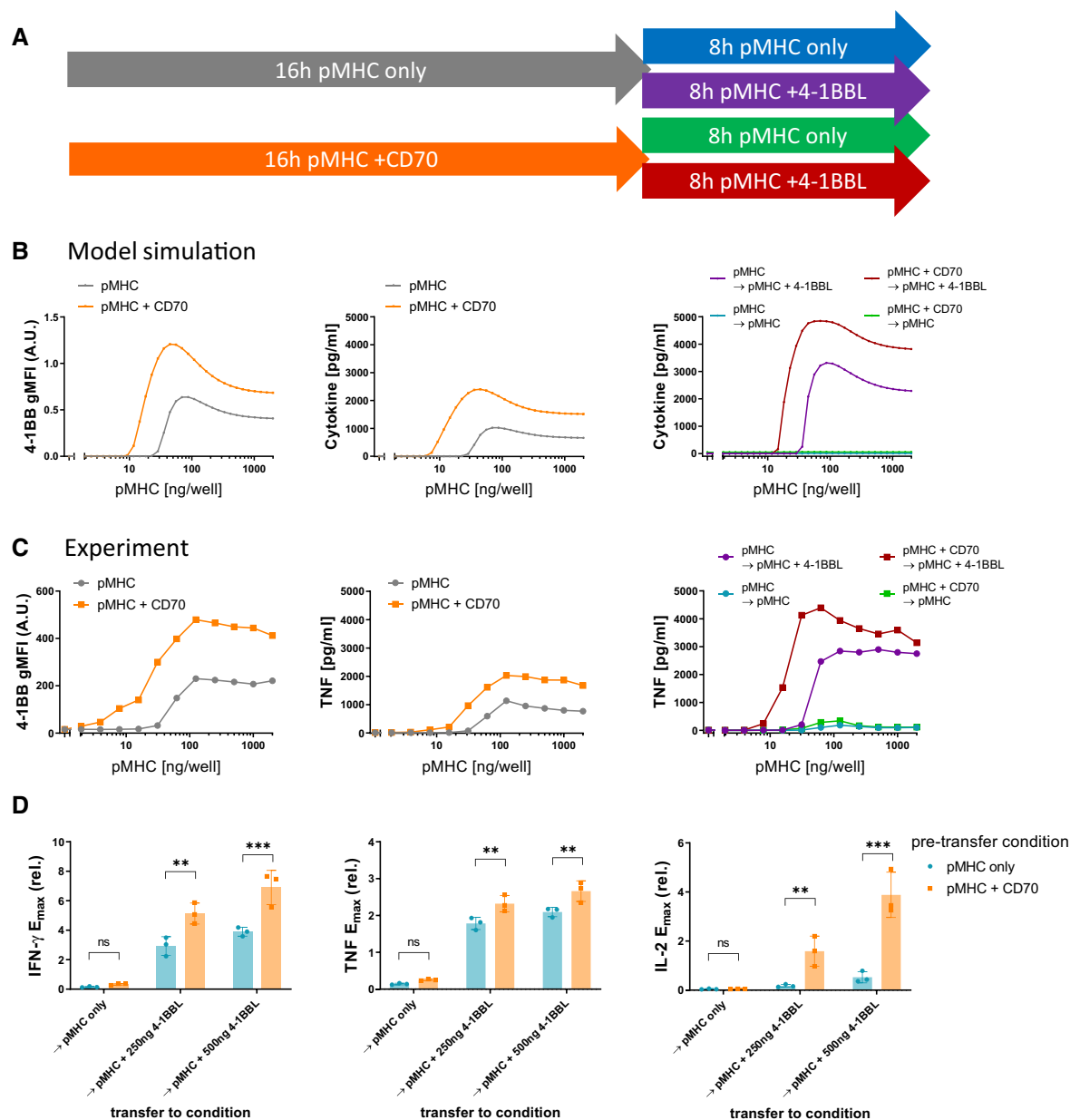D Simulated time courses of cytokine E_{max} in the absence or presence of CD70 or 4-1BBL.

Figure 5. Sequential co-stimulation through CD27 and 4-1BB exhibits synergy.

A   Overview of experiments to explore the impact of CD27 co-stimulation on subsequent 4-1BB co-stimulation.

B   Predictions of the operational model (as described in Fig 4) for the two-phase stimulation experiments shown in (A). 4-1BB expression (left) and cytokine response (middle) were simulated for a 16-h stimulation with pMHC only (grey) or presence of 200 ng/well CD70 (orange). Afterwards, the model predicted cytokine levels from these cells upon transfer to identical pMHC doses for another 8 h, with or without addition of 500 ng/well 4-1BBL (right).

C, D   Stimulation using primary human CD8^{+} T cells transduced with the c58/c61 TCR. The production of the cytokines IFN-γ, IL-2 and TNF into the culture medium supernatant was quantified by ELISA. (C) T-cell response during the first 16-h stimulation from one representative experiment (middle) and during the secondary 8-h stimulation from the same experiment (right). Cells from designated duplicate samples in the same experiment were stained with fluorescent anti-4-1BB antibodies after the first 16-h stimulation and analysed by flow cytometry (left). (D) E_{max} values from three separate repeats of the experiment were extracted from dose–response curve fits and normalised to the cytokine response without co-stimulation during the 16 h pre-stimulation (mean ± SD). Post-transfer conditions were compared using one-way ANOVA with Šídák's correction for multiple comparisons. ns (not significant) = P-value > 0.05; **P-value < 0.01; ***P-value < 0.001.

(Fig 5C and D). Since this synergy is based on the activation-induced expression of 4-1BB, other activation-induced co-stimulatory receptors should hypothetically behave similarly.

Indeed, we confirmed a similar synergy for GITR showing that IFN-γ production was significantly enhanced when T cells received early CD27 co-stimulation before GITR co-stimulation (Appendix Fig S9).

Discussion

In this study, we collected time series data with precisely titrated inputs in a minimal *in vitro* system to characterise the quantitative impact of TNFRSF co-stimulation on the T-cell cytokine response. We found that while both 4-1BB and CD27 co-stimulation increased efficacy of the response with minor increases in sensitivity, only 4-1BB was able to prolong the response duration. We found only minor changes in cytokine production by GITR and OX40 co-stimulation in this initial screen. These phenotypes were consistent with their surface expression dynamics, with CD27 being rapidly downregulated upon ligand engagement, whereas 4-1BB was upregulated by TCR signalling, which partially counteracted its ligand-induced downregulation. Both GITR and OX40 were induced with slower kinetics and to a lesser extent compared with 4-1BB. An operational model of T-cell activation could explain the different phenotypes of CD27 and 4-1BB by a shared signalling mechanism (lowering the TCR signalling threshold for cytokine production) but differences in the regulation of their surface expression.

This is consistent with the current molecular view that suggests conserved signalling pathways between TRAF-binding members of the TNFRSF. While they may utilise different TRAF variants, they are commonly strong activators of NF-κB and engage MAPK pathways (Chen & Flies, 2013), supporting a shared co-stimulation mechanism. TCR signalling is known to efficiently activate NFAT, while the other major transcription factors of T-cell activation, AP-1 (through the MAPKs ERK and JNK) and NF-κB, typically require stronger or prolonged stimulation (Macián *et al*, 2002; Wells, 2009; Marangoni *et al*, 2013). By supplementing AP-1 and NF-κB activation, it is thus plausible that co-stimulation through TNFRSF can lower the amount of TCR signalling required to elicit a response. Therefore, when T cells adapt to a pMHC stimulus by downregulating their TCR signalling machinery, sufficient co-stimulation would be able to revert this state of unresponsiveness.

Interestingly, other hyporesponsive T-cell phenotypes such as anergy and exhaustion are also characterised by diminished TCR signalling, either through downregulation of signalling molecules or expression of co-inhibitory receptors (Schwartz, 2003; Wherry, 2011). Moreover, imbalanced activation of transcription factors in favour of NFAT is also implicated in the induction of these states (Macián *et al*, 2002; Wells, 2009; Martinez *et al*, 2015), so it is not surprising that TNFRSF co-stimulation has been reported to counteract both anergy and exhaustion *in vivo* (Wilcox *et al*, 2004; Long *et al*, 2015; Zhao *et al*, 2015). However, a causal relationship of this effect with increase in NF-κB and AP-1 activation upon TNFRSF activation remains to be formally established.

The plate-based solid-phase stimulation system we have used offers the ability to independently vary the ligands to different surface receptors. However, a shortcoming of this system is that the presented ligands are immobile. In the case of IgSF co-signalling receptors, it has been demonstrated that co-clustering between receptors is important because cytoplasmic enzymes bound to one receptor modify another (Dushek *et al*, 2012; Hui *et al*, 2017; Suter *et al*, 2021). Although mobility is important for this receptor-proximal signal integration (Dushek *et al*, 2012), it is less clear whether it is important for co-signalling by TNFRSF members that integrate their signals more distally (Watts, 2005; Zapata *et al*, 2018).

While our coarse-grained "operational" model captures the signal-processing behaviour of the cell, it is unable to pinpoint molecular interactions between TCR and co-stimulatory signalling. Therefore, it should be seen as complement to molecular maps rather than their replacement (Antebi *et al*, 2017). One of the advantages of operational models is the capacity to produce predictions of T-cell responses to more complex inputs, such as combinations of co-stimulatory ligands. We experimentally validated the prediction of synergy between TNFRSF members that relied on the feedback regulation of the expression of 4-1BB and other inducible TNFRSF co-stimulatory receptors. In fact, CD27 is expressed on resting T cells and is rapidly downregulated upon ligand contact, whereas expression of the other TNFRSF members has variable kinetics and requires activation of the T cell to be induced, separating their primary time of action. Feedback regulation of the inducible TNFRSF members is thus possibly capable of imprinting a "history" of past activatory and co-stimulatory encounters, allowing even early co-stimulators such as CD27 to affect the later response long after they have been downregulated, if the appropriate ligands to inducible TNFRSF members are present.

Assuming that our observation is the result of feedback regulation of inducible co-stimulatory receptors expressed in proportion to the strength of T-cell activation, rather than immediate integration of signals from multiple receptors, this synergy is not necessarily exclusive to the TNFRSF. It is very likely that co-signalling receptors from other protein families can affect expression of inducible TNFRSF, as well. Based on similar observations of tightly regulated transient and temporally staggered expression of co-stimulatory and co-inhibitory receptors, Chen and colleagues have proposed a "tidal model", where immune cells at different stages of the response and their differentiation will be affected by different sets of co-signalling ligands (Zhu *et al*, 2011). Our data demonstrate that these changes can be highly dynamic, allowing for rapid fine-tuning on the time scale of hours. Although we have focused on CD8^{+} T cells, this fine-tuning is likely to operate for CD4^{+} T cells albeit with a different set of TNFRSF members (Appendix Fig S2) (Serghides *et al*, 2005; Yu *et al*, 2006; Clouthier *et al*, 2015).

Adoptive cell therapies using T cells expressing chimeric antigen receptor (CAR) are now routinely used in the clinic to treat B-cell malignancies. However, long-term remission is not achieved in a large fraction of patients and the therapy has yet to be proven in solid tumours (Mardiana *et al*, 2019; Martinez & Moon, 2019). Importantly, the ability of adoptively transferred CD8^{+} T-cell blasts to produce the cytokine IFN-γ is critical for tumour control (Boulch *et al*, 2021). Our model suggests that 4-1BB can be critical for the sustained production of IFN-γ when the TCR signalling machinery is downregulated as T cells adapt to a TCR stimulus. Therefore, inserting 4-1BB co-stimulatory domains directly into a CAR might limit its effectiveness, as CARs are also known to be downregulated upon triggering (Eyquem *et al*, 2017; Trendel *et al*, 2021), and we have shown that co-stimulatory receptors that are downregulated alongside the TCR (such as CD27) are unable to prevent unresponsiveness through adaptation. Targeted stimulation of endogenous 4-1BB and/or co-transduction of plasmids for the constitutive expression of CD27 or 4-1BB might provide a better way to enhance the potency of T cells used for adoptive cell therapy. In a direct comparison, T cells co-transduced with a second-generation CAR and 4-1BBL for co-stimulation in *cis* and *trans* have been shown to be

superior to third-generation CAR T cells *in vivo* (Zhao *et al*, 2015). Alternatively, 'armored' CAR T cells engineered to inducibly produce pro-inflammatory cytokines in order to adjust the tumour microenvironment in their favour have been proposed (Liu *et al*, 2019). Here, type-I interferons could be promising, since they are known to induce TNFSF ligands on APCs (Chang *et al*, 2017).

Co-signalling receptors are critically important regulators of T-cell responses, and currently, these receptors are largely classified into the binary categories of co-stimulation or co-inhibition (Chen & Flies, 2013). Using systematic experiments, we have been able to go beyond this binary classification by identifying different quantitative phenotypes induced by co-stimulation through different TNFR members. An operational model for how T-cell responses is regulated by the TCR allowed us to explore how different quantitative co-stimulation phenotypes can arise depending on where in the TCR signalling pathway a specific co-stimulation receptor integrates and how the surface expression of the co-stimulation receptor is regulated. Although these models lack molecular information, they can be helpful to provide mechanisms (how inputs are converted into outputs) and can make operational predictions (Lever *et al*, 2014; Antebi *et al*, 2017). Indeed, the model predicted how co-stimulation from one receptor (CD27) can impact subsequent co-stimulation from other receptors (4-1BB, GITR). By combining quantitative experiments and mathematical modelling, it may be possible to produce an operational map for how different surface receptors quantitatively control T-cell responses.

Materials and Methods

Reagents and Tools table

Reagent/resource	Reference or source	Identifier or Catalog Number
Experimental Models		
Primary CD8+ T cells from LRS (leukocyte reduction system) cones (*H. sapiens*)	NHS (National Health Services) Blood and Transplant	N/A
HEK293T	ATCC	CRL-3216
Recombinant DNA		
pELNS-1G4 c58/c61 (*affinity-enhanced TCR, identical with "1G4c113" in referred publication*)	Li *et al* (2005)	Adaptimmune
pRSV-Rev	Dull *et al* (1998)	Adaptimmune
pMDLg/pRRE	Dull *et al* (1998)	Prof. Dr. Harald Wajant, Universitätsklinikum Würzburg, Germany
pMD2.G	Dull *et al* (1998)	
pCR3-FLAG-TNC-4-1BBL	Wyzgol *et al* (2009)	
pCR3-FLAG-TNC-CD70	Wyzgol *et al* (2009)	Prof. Dr. Harald Wajant, Universitätsklinikum Würzburg, Germany
pCR3-FLAG-TNC-GITRL	Wyzgol *et al* (2009)	
pCR3-FLAG-TNC-OX40L	Müller *et al* (2008)	
Antibodies		
Mouse-anti-4-1BB (1:200)	BioLegend	309824
Mouse-anti-CD27 (1:200)	BioLegend	356432, 356406, 356418
Mouse-anti-GITRL (1:200)	Miltenyi	130-121-331
Mouse-anti-OX40L (1:200)	BioLegend	350018, 350014
Mouse-anti-HLA-A/B/C	Bio-Rad	MCA81
Goat-anti-mouse IgG (H + L) (polyclonal, 1:5,000)	LI-COR	926-32210
Mouse-anti-CD25 (1:200)	BioLegend	302630
Oligonucleotides and other sequence-based reagents		
Cloning adapter for insertion of AviTag into BamHI cut site of pCR3-FLAG-TNC-TNFSF constructs (forward)	This study (supplied by Invitrogen—Thermo Fisher)	5′−GATCCGGCCTGAACGATATTTTTGAAGCGCAGAAA ATTGAATGGCATGAAA−3′
Cloning adapter for insertion of AviTag into BamHI cut site of pCR3-FLAG-TNC-TNFSF constructs (reverse)	This study (supplied by Invitrogen – Thermo Fisher)	3′−GCCGGACTTGCTATAAAAACTTCGCGTCTTTTAAC TTACCGTACTTTCTAG−5′
Peptide for generation of high-affinity pMHC tetramers to the c58/c61 TCR ($K_D = 7.07 \times 10^{-11}$ M)	Lever *et al* (2016) (supplied by GenScript)	Amino acid sequence: SLLMWITQV

Reagents and Tools table (continued)

Reagent/resource	Reference or source	Identifier or Catalog Number
Peptide for generation of pMHC ligands to the c58/c61 TCR ($K_D = 1.78 \times 10^{-6}$ M)	Lever *et al* (2016) (supplied by GenScript)	Amino acid sequence: SLLAWITKV
Chemicals, Enzymes and other reagents		
ANTI-FLAG® M2 Affinity Gel	Sigma-Aldrich (now MilliporeSigma)	A2220-5ML
BamHI, with NEB CutSmart® Buffer	New England Biolabs	R0136L
BirA biotin-protein ligase bulk reaction kit	Avidity	https://www.avidity.com/commerce/product.asp?NUMBER=2
DMEM – high glucose	Sigma-Aldrich (now MilliporeSigma)	D5796
Dynabeads Human T-Activator CD3/CD28	Gibco™, Thermo Fisher Scientific	11132D
Foetal Bovine Serum (FBS)	Gibco™, Thermo Fisher Scientific	
Ficoll-Paque PLUS density gradient medium	GE Healthcare (now Cytiva)	17144003
Recombinant human IL-2	PeproTech	200-02
RetroNectin	Takara Bio	T100B
RPMI 1640	Sigma-Aldrich (now MilliporeSigma)	R8758
Streptavidin:RPE	Bio-Rad	STAR4A
T4 DNA ligase	Roche, Sigma-Aldrich (now MilliporeSigma)	10481220001
T4 polynucleotide kinase, with NEB T4 PNK Reaction Buffer	New England Biolabs	M0201S
X-tremeGene™ 9	Roche, Sigma-Aldrich (now MilliporeSigma)	6365809001
Software		
BD FACSDiva v8.0	https://www.bdbiosciences.com/en-us/products/software/instrument-software/bd-facsdiva-software#Overview	
FlowJo v10	https://www.flowjo.com/	
GraphPad Prism 8	https://www.graphpad.com/	
MATLAB R2018b	https://www.mathworks.com/products/matlab.html	
Other		
BD LSRFortessa X-20	BD	
SpectraMax M5	Molecular Devices	
Pierce™ Streptavidin Coated High Capacity 96-well Plates	Thermo Fisher	15500
Human IFN gamma Uncoated ELISA Kits	Thermo Fisher	88-7316-77
Human IL-2 Uncoated ELISA Kits	Thermo Fisher	88-7025-77
Human TNF alpha Uncoated ELISA Kits	Thermo Fisher	88-7346-77
RosetteSep™ Human CD4+ T Cell Enrichment Cocktail	Stemcell	15062
RosetteSep™ Human CD8+ T Cell Enrichment Cocktail	Stemcell	15063

Methods and Protocols

Protein production

pMHCs were refolded *in vitro* from the extracellular residues 1–287 of the HLA-A*02:01 α-chain, β2-microglobulin and NY-ESO-1157-165 peptide variant SLLAWITKV as described previously (Lever *et al*, 2016). TNFSF ligand expression constructs were a kind gift from Harald Wajant (Würzburg, Germany) and contained a Flag tag for the purification and a tenascin-C trimerisation domain (Müller *et al*, 2008; Wyzgol *et al*, 2009). We added an N-terminal AviTag as biotinylation site using standard cloning techniques. The protein was produced by transient transfection of HEK 293T cells with X-tremeGENE HP Transfection Reagent (Roche), according to the manufacturer's instructions, and purified following a published protocol (Wyzgol *et al*, 2009), with the exception of the elution step in which we used acid elution with 0.1 M glycine-HCl at pH 3.5. The pMHC or co-stimulatory ligand was then biotinylated *in vitro* by BirA enzyme, according to the manufacturer's instructions (Avidity

Biosciences), purified using size-exclusion chromatography with HBS-EP (pH 7.4, 10 mM HEPES, 150 mM NaCl, 3 mM EDTA and 0.005% v/v Tween20) as flow buffer and stored in aliquots at −80°C.

Production of lentiviral particles for transduction

HEK 293T cells were seeded into six-well plates before transfection to achieve 50–80% confluency on the day of transfection. Cells were co-transfected with the respective third-generation lentiviral transfer vectors and packaging plasmids using Roche X-tremeGENE HP (0.8 µg lentiviral expression plasmid, 0.95 µg pRSV-Rev, 0.37 µg pMD2.G, 0.95 µg pMDLg/pRRE per well) (Dull *et al*, 1998). The supernatant was harvested and filtered through a 0.45 µm cellulose acetate filter 24–36 h later. The affinity-matured c58c61 (Li *et al*, 2005) was used in a standard third-generation lentiviral vector with the human EF1α promoter.

T-cell isolation and culture

Up to 50 ml peripheral blood was collected by a trained phlebotomist from healthy volunteer donors after informed consent had been taken. This project has been approved by the Medical Sciences Interdivisional Research Ethics Committee of the University of Oxford (R51997/RE001), and all samples were anonymised in compliance with the Data Protection Act. Alternatively, leukocyte cones were purchased from National Health Services Blood and Transplant service. Only HLA-A2-peripheral blood or leukocyte cones were used because of the cross-reactivity of the high-affinity receptors used in this project, which leads to fratricide of HLA-A2$^+$ T cells (Tan *et al*, 2015). CD8$^+$ T cells were isolated directly from blood using the CD8$^+$ T Cell Enrichment Cocktail (STEMCELL Technologies) and density gradient centrifugation according to manufacturer's instructions. The isolated CD8$^+$ T cells were washed and resuspended at a concentration of 1×10^6 cells/ml in culture medium (RPMI 1640 with 10% foetal bovine serum, 100 units penicillin and 100 µg streptomycin per ml) supplemented with 50 U/ml IL-2 and 1×10^6 CD3/CD28-coated Human T-Activator Dynabeads/ml (Life Technologies). The next day, 1×10^6 T cells were transduced with the 2.5 ml virus-containing supernatant from one well of HEK 293T cells, supplemented with 50 U/ml of IL-2. The medium was replaced with fresh culture medium containing 50 U/ml IL-2 every 2–3 days. CD3/CD28-coated beads were removed on day 5 after lentiviral transduction, and the cells were used for experiments on days 10–14. TCR expression was assessed by staining with NY-ESO 9V PE-conjugated tetramer (inhouse produced using refolded HLA*A02:01 with NY-ESO-1$_{157-165}$ 9V and streptavidin-PE [Bio-Rad AbD Serotec or BioLegend]) using flow cytometry.

T-cell stimulation

T cells were stimulated with titrations of plate-immobilised pMHC ligands with or without co-immobilised ligands for accessory receptors. Ligands were diluted to the working concentrations in sterile PBS. 50 µl serially diluted pMHC were added to each well of high-binding capacity streptavidin-coated 96-well plates (#15500; Thermo Fisher Scientific). After a minimum 45-min incubation at room temperature, the plates were washed with sterile PBS. Where accessory receptor ligands were used, those were similarly diluted and added to the plate for a second incubation. After washing the stimulation plate with PBS, 7.5×10^4 T cells were added in 200 µl culture medium (RPMI 1640 with 10% foetal bovine serum, 100 units penicillin and 100 µg streptomycin per ml) without IL-2 to each stimulation condition. The plates were spun at 50–100 *g* for 1 min to settle down the cells and then incubated at 37°C with 5% CO$_2$. At the indicated time points of the stimulation experiments, cells were harvested by pipetting and transferred to V-bottom 96-well plates. The harvested cells were pelleted (5 min at 520 *g*) and processed for flow cytometry, and the supernatants were collected for ELISAs. To stimulate T cells in two phases with different conditions, stimulation plates for a second condition were prepared as described above. At the time point of transfer between conditions, cells were harvested, pelleted in V-bottom 96-well plates and subsequently resuspended in fresh prewarmed culture medium (200 µl/well) before transferring them to the prepared stimulation plates for the second phase. To settle down the cells again, plates were briefly spun at 50–100 *g* for 1 min and returned to the incubator (37°C/5% CO$_2$) for the specified times.

Flow cytometry

Flow cytometry was used to quantify surface expression of TCR, co-stimulatory receptors and activation markers at specified time points and at the end of stimulation experiments. Harvested cells were pelleted in V-bottom 96-well plates (5 min at 520 *g*) and kept on ice during the staining procedure. The pellets were resuspended in staining buffer (PBS with 1% BSA) containing fluorescently labelled pMHC tetramers and/or fluorophore-conjugated antibodies (Table in Reagents and Tools table) at previously titrated working concentrations (usually 1:200 for commercially available antibodies from BioLegend). After 20 min, cells were washed twice with staining buffer (200 µl/well, 5 min at 520 *g*) and resuspended in 80 µl/well PBS for flow cytometry. Samples were analysed on a BD FACSCalibur™ or BD LSRFortessa™ X-20 with a BD High Throughput Sampler for automated acquisition. Flow cytometry data were analysed in FlowJo V10.

ELISA

After harvesting the cells from the stimulation experiments, the supernatants were separated from the cell pellets, collected in round-bottom 96-well plates and kept on ice for short-term storage (< 12 h). To quantify the cytokines IFN-γ, IL-2 and TNF, ELISAs were performed using Nunc MaxiSorp™ flat-bottom 96-well plates and the respective Invitrogen™ Uncoated ELISA Kits (Thermo Fisher Scientific) according to the manufacturer's protocol. A BioTek ELx405 plate washer was used for washing steps, and absorbance at 450 and 570 nm was measured using a SpectraMax M5 plate reader (Molecular Devices). Standards in duplicates were included for each plate to generate calibration curves for the calculation of cytokine concentrations.

Data analysis

We fit the following bell-shaped function to each dose–response curve using the function *lsqcurvefit* in MATLAB (MathWorks, MA),

$$y = E_{\min} + \frac{a + \frac{b-a}{1+\left(\frac{c_1}{x}\right)^{n_1}} - E_{\min}}{1 + \left(\frac{c_2}{x}\right)^{n_2}}.$$

We then used the smooth line produced by this function with 10,000 points to directly calculate the maximum amount of cytokine produced across different pMHC concentrations ($E_{\max}$) and the pMHC concentration producing the half-maximal response (EC$_{50}$) for

each dose–response curve (Appendix Fig S1A). We note that these are not fitted parameters but rather metrics determined directly from the line produced by the bell-shaped function. In certain cases, the cytokine response was so weak that the technical noise in the ELISA made it unfeasible to accurately estimate the EC_{50}. Therefore, EC_{50} values were excluded for dose responses where the fit E_{max} was below 50 pg/ml, which was usually the case for IL-2 at late time points. To further minimise the contribution of technical variability between experiments (originating, for instance, from differences in quality of stimulatory ligands, transduction efficiency of the cells and donor variability) the extracted absolute E_{max} and EC_{50} values were normalised to the mean E_{max} and EC_{50} values of each readout across all conditions in each experiment. Therefore, pooled and averaged E_{max} and EC_{50} values were not plotted as absolute values but as relative fold-change compared to one standard condition (e.g. pMHC without co-stimulation), as indicated for each figure. Statistical tests with appropriate corrections for multiple testing were performed as indicated for each figure in GraphPad Prism 8.

Mathematical modelling

We have used a mathematical model of pMHC binding to the TCR that induces both TCR downregulation and digital cytokine activation. The model presented in this work is a simplified version of a model we have recently described (Trendel *et al*, 2021). The model is represented by a system of ordinary differential equations (ODEs). Reaction rates in the model are described by mass-action kinetics with the exception of receptor-ligand binding, which is simplified under the assumption that equilibrium is reached rapidly (s to min) compared with the time scale of the experiments (hours), and the digital behaviour of TCR signalling described by an error function erf to account for natural variability of the activation threshold within the cell population. The model was numerically integrated using the solver *ode23s* in MATLAB (MathWorks, MA). The following set of ordinary differential equations describes the base model:

$$\frac{d(\text{TCR})}{dt} = k_1(1 - \text{TCR}) - k_2 * C$$

$$\frac{d(\text{Signal})}{dt} = \frac{1}{2} + \frac{1}{2}\,\text{erf}\left(\frac{C - \mu}{\sqrt{2}\sigma}\right) - k_3 * \text{Signal}$$

$$\frac{d(\text{Cytokine})}{dt} = k_4 * \text{Signal}.$$

Here, the parameter μ is the mean activation threshold in a population of T cells, σ is its standard deviation of μ in the population, and C is the amount of pMHC-TCR complexes,

$$C = \frac{\text{pMHC}^n}{\left(\frac{1}{K_A}\right)^n + \text{pMHC}^n} * \text{TCR}$$

where K_A is the affinity and n is the hill number. The surface expression of co-stimulatory receptors was modelled as follows:

$$\frac{d(\text{CD27})}{dt} = k_5(1 - \text{CD27}) - k_6 * \frac{\text{CD70}}{K_{D_{CD27}} + \text{CD70}} * \text{CD27}$$

$$\frac{d(41BB)}{dt} = k_7 * \text{Signal} - k_8 * \frac{41BBL}{K_{D_{41BB}} + 41BBL} * 41BB - k_9 * 41BB.$$

Under the assumption that co-stimulation through CD27 and 4-1BB affect the T-cell response by modulating the activation threshold, the equation for the integrated signal changes as follows:

$$\frac{d(\text{Signal})}{dt}$$

$$= \frac{1}{2} + \frac{1}{2}\,\text{erf}[\frac{1}{\sqrt{2}\sigma}((1 + k_{10} * \frac{\text{CD70}}{K_{D_{CD27}} + \text{CD70}}$$

$$+ k_{11} * \frac{41BBL}{K_{D_{41BB}} + 41BBL}]C - \mu)) - k_3 * \text{Signal}.$$

The parameter values for the generation of Figs 4 and 5 using this assumption are listed in Appendix Table S1.

The six alternative models for the CD27 co-stimulation transfer experiments in Appendix Fig S8 were simulated with the following equations, respectively, that were altered from the base model (above) to integrate co-stimulation at a different position:

$$\frac{d(\text{Signal})}{dt} =$$

$$\frac{1}{2} + \frac{1}{2}\,\text{erf}\left[\frac{1}{\sqrt{2}\sigma}\left(\left(1 + k_{10} * \frac{\text{CD70}}{K_{D_{CD27}} + \text{CD70}}\right)C - \mu\right)\right] - k_3 * \text{Signal} \quad (1)$$

$$\frac{d(\text{Signal})}{dt} = \frac{1}{2} + \frac{1}{2}\left(1 + k_{10} * \frac{\text{CD70}}{K_{D_{CD27}} + \text{CD70}}\right)\text{erf}\left(\frac{C - \mu}{\sqrt{2}\sigma}\right) - k_3 * \text{Signal} \quad (2)$$

$$\frac{d(\text{Signal})}{dt} = \frac{1}{2} + \frac{1}{2}\,\text{erf}\left(\frac{C - \mu}{\sqrt{2}\sigma}\right) + k_{10} * \frac{\text{CD70}}{K_{D_{CD27}} + \text{CD70}} - k_3 * \text{Signal} \quad (3)$$

$$\frac{d(\text{Signal})}{dt} = \frac{1}{2} + \frac{1}{2}\,\text{erf}\left(\frac{C - \mu}{\sqrt{2}\sigma}\right) - \frac{k_3 * \text{Signal}}{k_{10} * \frac{\text{CD70}}{K_{D_{CD27}} + \text{CD70}}} \quad (4)$$

$$\frac{d(\text{Cytokine})}{dt} = k_4 * \left(1 + k_{10} * \frac{\text{CD70}}{K_{D_{CD27}} + \text{CD70}}\right) * \text{Signal} \quad (5)$$

$$\frac{d(\text{Cytokine})}{dt} = k_4 * \text{Signal} + k_{10} * \frac{\text{CD70}}{K_{D_{CD27}} + \text{CD70}} \quad (6)$$

Data availability

This study includes no data deposited in external repositories. The raw data generated in this study are provided as source data.

Expanded View for this article is available online.

Author contributions

Contributor Roles Taxonomy (CRediT): JN, PK and OD conceptualised the study; JN and OD contributed to methodology; JN and OD involved in formal analysis; JN, JP and PK investigated the study; JN curated the data; JN and OD wrote—original draft; JN, JP, PK and OD wrote—review & editing; JN and OD produced visuals; OD supervised/project administration/funded the study.

Conflict of interest

The authors declare that they have no conflict of interest.

References

Abu-Shah E, Trendel N, Kruger P, Nguyen J, Pettmann J, Kutuzov M, Dushek O (2020) Human CD8 + T cells exhibit a shared antigen threshold for different effector responses. *J Immunol* 205: 1503–1512

Aleksic M, Dushek O, Zhang H, Shenderov E, Chen J-L, Cerundolo V, Coombs D, van der Merwe PA (2010) Dependence of T cell antigen recognition on T cell receptor-peptide MHC confinement time. *Immunity* 32: 163–174

Ansell SM, Flinn I, Taylor MH, Sikic BI, Brody J, Nemunaitis J, Feldman A, Hawthorne TR, Rawls T, Keler T *et al* (2020) Safety and activity of varlilumab, a novel and first-in-class agonist anti-CD27 antibody, for hematologic malignancies. *Blood Adv* 4: 1917–1926

Antebi YE, Linton JM, Klumpe H, Bintu B, Gong M, Su C, McCardell R, Elowitz MB (2017) Combinatorial signal perception in the BMP pathway. *Cell* 170: 1184–1196.e24

Bachmann MF, Mckall-faienza K, Schmits R, Bouchard D, Beach J, Speiser DE, Mak TW, Ohashi PS (1997) Distinct Roles for LFA-1 and CD28 during activation of naive T cells: adhesion versus costimulation. *Immunity* 7: 549–557

Bachmann MF, Ohashi PS (1999) The role of T-cell receptor dimerization in T-cell activation. *Immunol Today* 20: 568–576

Boulch M, Cazaux M, Loe-Mie Y, Thibaut R, Corre B, Lemaître F, Grandjean CL, Garcia Z, Bousso P (2021) A cross-talk between CAR T cell subsets and the tumor microenvironment is essential for sustained cytotoxic activity. *Sci Immunol* 6: 1–17

Bucy RP, Panoskaltsis-Mortari A, Huang GQ, Li J, Karr L, Ross M, Russell JH, Murphy KM, Weaver CT (1994) Heterogeneity of single cell cytokine gene expression in clonal T cell populations. *J Exp Med* 180: 1251–1262

Chang YH, Wang KC, Chu KL, Clouthier DL, Tran AT, Torres Perez MS, Zhou AC, Abdul-Sater AA, Watts TH (2017) Dichotomous expression of TNF superfamily ligands on antigen-presenting cells controls post-priming anti-viral CD4+T cell immunity. *Immunity* 47: 943–958.e9

Chen L, Flies DB (2013) Molecular mechanisms of T cell co-stimulation and co-inhibition. *Nat Rev Immunol* 13: 227–242

Choi BK, Kim YH, Choi JH, Kim CH, Kim KS, Sung YC, Lee YM, Moffett JR, Kwon BS (2011) Unified immune modulation by 4–1BB triggering leads to diverse effects on disease progression in vivo. *Cytokine* 55: 420–428

Clouthier DL, Zhou AC, Wortzman ME, Luft O, Levy GA, Watts TH (2015) GITR intrinsically sustains early type 1 and late follicular helper CD4 T cell accumulation to control a chronic viral infection. *PLoS Pathog* 11: 1–21

Dull T, Zufferey R, Kelly M, Mandel RJ, Nguyen M, Trono D, Naldini L (1998) A third-generation lentivirus vector with a conditional packaging system. *J Virol* 72: 8463–8471

Dushek O, Aleksic M, Wheeler R, Zhang H, Cordoba S, Peng Y, Chen J, Cerundolo V, Dong T, Coombs D *et al* (2011) Antigen potency and maximal efficacy reveal a mechanism of efficient T cell activation. *Sci Signal* 4: ra39

Dushek O, Goyette J, van der Merwe PA (2012) Non-catalytic tyrosine-phosphorylated receptors. *Immunol Rev* 250: 258–276

Eyquem J, Mansilla-Soto J, Giavridis T, Van Der Stegen SJ, Hamieh M, Cunanan KM, Odak A, Gönen M, Sadelain M (2017) Targeting a CAR to the TRAC locus with CRISPR/Cas9 enhances tumour rejection. *Nature* 543: 113–117

Gramaglia I, Weinberg AD, Lemon M, Croft M (1998) Ox-40 ligand: a potent costimulatory molecule for sustaining primary CD4 T cell responses. *J Immunol (Baltimore, Md.:1950)* 161, 6510–6517

Han S, Asoyan A, Rabenstein H, Nakano N, Obst R (2010) Role of antigen persistence and dose for CD4+ T-cell exhaustion and recovery. *Proc Natl Acad Sci USA* 107: 20453–20458

Huang J, Brameshuber M, Zeng X, Xie J, Li Q-J, Chien Y-H, Valitutti S, Davis M (2013) A single peptidemajor histocompatibility complex ligand triggers digital cytokine secretion in CD4+ T Cells. *Immunity* 39: 846–857

Hui E, Cheung J, Zhu J, Su X, Taylor MJ, Wallweber HA, Sasmal DK, Huang J, Kim JM, Mellman I *et al* (2017) T cell costimulatory receptor CD28 is a primary target for PD-1–mediated inhibition. *Science* 355: 1428–1433

Iezzi G, Karjalainen K, Lanzavecchia A (1998) The duration of antigenic stimulation determines the fate of naive and effector T cells. *Immunity* 8: 89–95

Koyasu S, Lawton T, Novick D, Recny MA, Siliciano RF, Wallner BP, Reinherz EL (1990) Role of interaction of CD2 molecules with lymphocyte function-associated antigen 3 in T-cell recognition of nominal antigen. *Proc Natl Acad Sci* 87: 2603–2607

Langenhorst D, Haack S, Göb S, Uri A, Lühder F, Vanhove B, Hünig T, Beyersdorf N (2018) CD28 costimulation of T helper 1 cells enhances cytokine release in vivo. *Front Immunol* 9: 1–13

Lever M, Maini PK, van der Merwe PA, Dushek O (2014) Phenotypic models of T cell activation. *Nat Rev Immunol* 14: 619–629

Lever M, Lim H-S, Kruger P, Nguyen J, Trendel N, Abu-Shah E, Maini PK, van der Merwe PA, Dushek O (2016) A minimal signalling architecture explains the T cell response to a 1,000,000-fold variation in antigen affinity and dose. *Proc Natl Acad Sci USA* 113: E6630–E6638

Li Y, Moysey R, Molloy PE, Vuidepot A-L, Mahon T, Baston E, Dunn S, Liddy N, Jacob J, Jakobsen BK *et al* (2005) Directed evolution of human T-cell receptors with picomolar affinities by phage display. *Nat Biotechnol* 23: 349–354

Liu X, Wang Y, Lu H, Li J, Yan X, Xiao M, Hao J, Alekseev A, Khong H, Chen T *et al* (2019) Genome-wide analysis identifies NR4A1 as a key mediator of T cell dysfunction. *Nature* 567: 525–529

Locke FL, Ghobadi A, Jacobson CA, Miklos DB, Lekakis LJ, Oluwole OO, Lin YI, Braunschweig I, Hill BT, Timmerman JM *et al* (2019) Long-term safety and activity of axicabtagene ciloleucel in refractory large B-cell lymphoma (ZUMA-1): a single-arm, multicentre, phase 1–2 trial. *Lancet Oncol* 20: 31–42

Long AH, Haso WM, Shern JF, Wanhainen KM, Murgai M, Ingaramo M, Smith JP, Walker AJ, Kohler ME, Venkateshwara VR *et al* (2015) 4-1BB costimulation ameliorates T cell exhaustion induced by tonic signaling of chimeric antigen receptors. *Nat Med* 21, 581–590

Macián F, García-Cózar F, Im SH, Horton HF, Byrne MC, Rao A (2002) Transcriptional mechanisms underlying lymphocyte tolerance. *Cell* 109: 719–731

Marangoni F, Murooka TT, Manzo T, Kim EY, Carrizosa E, Elpek NM, Mempel TR (2013) The transcription factor NFAT exhibits signal memory during

serial T cell interactions with antigen-presenting cells. *Immunity* 38: 237−249

Mardiana S, Solomon BJ, Darcy PK, Beavis PA (2019) Supercharging adoptive T cell therapy to overcome solid tumor−induced immunosuppression. *Sci Transl Med* 11https://doi.org/10.1126/scitranslmed.aaw2293

Martinez GJ, Pereira RM, Äijö T, Kim EY, Marangoni F, Pipkin ME, Togher S, Heissmeyer V, Zhang YC, Crotty S *et al* (2015) The transcription factor NFAT promotes exhaustion of activated CD8+ T cells. *Immunity* 42: 265−278

Martinez M, Moon EK (2019) CAR T cells for solid tumors: new strategies for finding, infiltrating, and surviving in the tumor microenvironment. *Front Immunol* 10: 128

van der Merwe PA, Dushek O (2011) Mechanisms for T cell receptor triggering. *Nat Rev Immunol* 11: 47−55

Müller N, Wyzgol A, Münkel S, Pfizenmaier K, Wajant H (2008) Activity of soluble OX40 ligand is enhanced by oligomerization and cell surface immobilization. *FEBS J* 275: 2296−2304

Ramakrishna V, Sundarapandiyan K, Zhao B, Bylesjo M, Marsh HC, Keler T (2015) Characterization of the human T cell response to in vitro CD27 costimulation with varlilumab. *J Immunother Cancer* 3: 1−13

Rapoport AP, Stadtmauer EA, Binder-Scholl GK, Goloubeva O, Vogl DT, Lacey SF, Badros AZ, Garfall A, Weiss B, Finklestein J *et al* (2015) NY-ESO-1-specific TCR-engineered T cells mediate sustained antigen-specific antitumor effects in myeloma. *Nat Med* 21: 914−921

Schaer DA, Hirschhorn-Cymerman D, Wolchok JD (2014) Targeting tumor-necrosis factor receptor pathways for tumor immunotherapy. *J Immunother Cancer* 2: 1−9

Schwartz RH (2003) T cell anergy. *Ann Rev Immunol* 21, 305−334

Serghides L, Bukczynski J, Wen T, Wang C, Routy J-P, Boulassel M-R, Sekaly R-P, Ostrowski M, Bernard NF, Watts TH (2005) Evaluation of OX40 ligand as a costimulator of human antiviral memory CD8 T cell responses: comparison with B7.1 and 4−1BBL. *J Immunol* 175: 6368−6377

Singh NJ, Schwartz RH (2003) The strength of persistent antigenic stimulation modulates adaptive tolerance in peripheral CD4+ T Cells. *J Exp Med* 198: 1107−1117

Smith-Garvin JE, Koretzky GA, Jordan MS (2009) T cell activation. *Annu Rev Immunol* 27: 591−619

Stamou P, de Jersey J, Carmignac D, Mamalaki C, Kioussis D, Stockinger B (2003) Chronic exposure to low levels of antigen in the periphery causes reversible functional impairment correlating with changes in CD5 levels in monoclonal CD8 T Cells. *J Immunol* 171: 1278−1284

Stauber DJ, Debler EW, Horton PA, Smith KA, Wilson IA (2006) Crystal structure of the IL-2 signaling complex: paradigm for a heterotrimeric cytokine receptor. *Proc Natl Acad Sci USA* 103: 2788−2793

Suter EC, Schmid EM, Harris AR, Voets E, Francica B, Fletcher DA (2021) Antibody:CD47 ratio regulates macrophage phagocytosis through competitive receptor phosphorylation. *Cell Rep* 36: 109587

Tan MP, Gerry AB, Brewer JE, Melchiori L, Bridgeman JS, Bennett AD, Pumphrey NJ, Jakobsen BK, Price DA, Ladell K *et al* (2015) T cell receptor binding affinity governs the functional profile of cancer-specific CD8+ T cells. *Clin Exp Immunol* 180: 255−270

Tolcher AW, Sznol M, Hu-Lieskovan S, Papadopoulos KP, Patnaik A, Rasco DW, Di Gravio D, Huang B, Gambhire D, Chen Y *et al* (2017) Phase Ib study of utomilumab (PF-05082566), a 4−1BB/CD137 agonist, in combination with pembrolizumab (MK-3475) in patients with advanced solid tumors. *Clin Cancer Res* 23: 5349−5357

Trendel N, Kruger P, Gaglione S, Nguyen J, Pettmann J, Sontag ED, Dushek O (2021) Perfect adaptation of CD8+ T cell responses to constant antigen input over a wide range of affinity is overcome by costimulation. *Sci Signal* 14 https://doi.org/10.1126/scisignal.aay9363

Viola A, Lanzavecchia A (1996) T cell activation determined by T cell receptor number and tunable thresholds. *Science (New York, NY)* 273: 104−106

Wagner J, Wickman E, DeRenzo C, Gottschalk S (2020) CAR T cell therapy for solid tumors: bright future or dark reality? *Mol Ther* 28: 2320−2339

Wang X, Rickert M, Garcia KC (2005) Structural biology: structure of the quaternary complex of interleukin-2 with its α, β and γc receptors. *Science* 310: 1159−1163

Ward-Kavanagh LK, Lin WW, Šedý JR, Ware CF (2016) The TNF receptor superfamily in co-stimulating and co-inhibitory responses. *Immunity* 44: 1005−1019

Watts TH (2005) TNF/TNFR family members in costimulation of T cell responses. *Annu Rev Immunol* 23: 23−68

Weinkove R, George P, Dasyam N, McLellan AD (2019) Selecting costimulatory domains for chimeric antigen receptors: functional and clinical considerations. *Clin Transl Immunol* 8: 1−14

Wells AD (2009) New insights into the molecular basis of T cell anergy: anergy factors, avoidance sensors, and epigenetic imprinting. *J Immunol* 182: 7331−7341

Wherry EJ (2011) T cell exhaustion. *Nat Immunol* 12: 492−499.

Wilcox RA, Tamada K, Flies DB, Zhu G, Chapoval AI, Blazar BR, Kast WM, Chen L (2004) Ligation of CD137 receptor prevents and reverses established anergy of CD8+ cytolytic T lymphocytes *in vivo*. *Blood* 103: 177−184

Wyzgol A, Müller N, Fick A, Munkel S, Grigoleit GU, Pfizenmaier K, Wajant H (2009) Trimer stabilization, oligomerization, and antibody-mediated cell surface immobilization improve the activity of soluble trimers of CD27L, CD40L, 41BBL, and glucocorticoid-induced TNF receptor ligand. *J Immunol* 183: 1851−1861

Yu Q, Yue FY, Gu XX, Schwartz H, Kovacs CM, Ostrowski MA (2006) OX40 Ligation of CD4 + T cells enhances virus-specific CD8+ T cell memory responses independently of IL-2 and CD4 + T regulatory cell inhibition. *J Immunol* 176: 2486−2495

Zapata JM, Perez-Chacon G, Carr-Baena P, Martinez-Forero I, Azpilikueta A, Otano I, Melero I (2018) CD137 (4-1BB) signalosome: complexity is a matter of TRAFs. *Front Immunol* 9 https://doi.org/10.3389/fimmu.2018.02618

Zhang J, Bárdos T, Li D, Gál I, Vermes C, Xu J, Mikecz K, Finnegan A, Lipkowitz S, Glant TT (2002) Cutting edge: regulation of T cell activation threshold by CD28 costimulation through targeting Cbl-b for ubiquitination. *J Immunol* 169: 2236−2240

Zhao Z, Condomines M, van der Stegen SJ, Perna F, Kloss CC, Gunset G, Plotkin J, Sadelain M (2015) Structural design of engineered costimulation determines tumor rejection kinetics and persistence of CAR T cells. *Cancer Cell* 28: 415−428

Zhu Y, Yao S, Chen L (2011) Cell surface signaling molecules in the control of immune responses: a tide model. *Immunity* 34: 466−478